

MESO-FE MODELLING OF TEXTILE COMPOSITES: ROAD MAP, DATA FLOW AND ALGORITHMS

Stepan V. Lomov*, Dmitry S. Ivanov*, Ignaas Verpoest*

Masaru Zako**, Tetsusei Kurashiki**, Hiroaki Nakai**, Satoru Hirosawa**

*Department of Metallurgy and Materials Engineering, Katholieke Universiteit Leuven

**Graduate School of Engineering, Osaka University

Keywords: *textile composites; meso-modelling; internal geometry; micro-mechanics; finite elements; multi-level analysis*

Abstract

The paper discusses stages of the meso-FE analysis of a unit cell of an impregnated textile reinforcement and proposes a succession of steps ("road map") and the corresponding algorithms for it: (1) Building a model of internal geometry of the reinforcement; (2) Transferring the geometry into a volume description ("solid" CAD-model); (3) Preparation for meshing; correction of the interpenetration of volumes of yarns in the solid model and providing space for the thin matrix layers between the yarns; (4) Meshing; (5) Assigning local material properties of the impregnated yarns and the matrix; (6) Definition of the minimum possible unit cell using symmetry of the reinforcement and assigning periodic boundary conditions; (7) Homogenisation procedure; (8) Damage initiation criteria; (9) Damage propagation modelling. The "road map" is illustrated by examples of meso-FE analysis of woven and braided composites

1 Introduction

Textile composites are structured, hierarchical materials, having three structural levels:

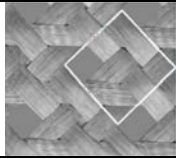
1. The macro(M)-level defines the 3D geometry of the composite part and the distribution of local reinforcement properties. The latter is connected to the former, as local parameters of the reinforcement (such as fibre volume fraction, reinforcement thickness and shear angle, hence local composite stiffness) are defined by the draping process during forming of the part. "Local" on the M-level means averaging (homogenisation) of the properties on the scale of one or several adjacent unit cells of the material, and corresponds to

"global" on the meso-level. "Global" on the M-level means overall loading conditions of the part.

2. The meso(m)-level defines the internal structure of the reinforcement and variations of the fibre direction and the fibre volume fraction inside the yarns and the fibrous plies. The internal structure is defined by the reinforcement textile architecture and deformations applied to the reinforcement during the part forming. "Local" on m-level means averaging (homogenisation) on the scale of several fibres (representative volume element (RVE) for fibre packing inside the yarn) of properties as fibre direction, fibre volume fraction and stiffness of the impregnated yarn. "Global" on the m-level means "local" on the M-level.

3. The micro(μ)-level defines the arrangement of the fibres in the RVE of the impregnated yarn or fibrous ply. "Local" data on μ -level are properties of fibres, matrix and their interface. Homogenised, "global" parameters are used as "local" data on the m-level.

Table 1 Parameters of the 3-axial braided composite

Parameter	Value
Braiding pattern	
Areal density, g/m ²	600
Braiding angle, °	90
Unit cell size (square shape), mm	14.4
Carbon tows	HTS 5631 Tenax 24K
Fibre diameter, μ m	7
Matrix	Epicote 828 LV/Epicure DX 6514
Fibre volume fraction, %	44

This paper deals with meso-level analysis of mechanical behaviour of textile composites, i.e.

textile reinforcement impregnated by a solid matrix. The bibliography of the subject is vast; we omit the references to the previous work of different researchers here for the reasons of the limited space of the paper. The reader is referred to [1] for a comprehensive review. Whilst similar issues could be considered for FE modelling of deformations of permeability of dry textile, these topics are out of scope of the present paper.

This paper uses the following software tools: textile geometry modelling software *WiseTex* [2] two general-purpose FE packages: the commercial ANSYS software and a package SACOM, developed by M.Zako in Osaka University in the 90-ies and extensively used by the Osaka group of the present authors for a wide spectrum of research topics. The general discussion is illustrated by an example of meso-FE analysis of 3-axial braided composite (Table 1).

2 Stages of meso-FE modelling

Consider a typical problem of meso-FE modelling of a unit cell of textile composite under loading conditions representing its actual loading in a composite part. The following tasks can be performed (Fig. 1a):

- For the given applied loading (which may include also thermal and cure stresses) calculate the stress-strain fields inside the unit cell;
 - Assess stress-strain concentrations and identify damage sites;
 - When damage occurs, recalculate the local mechanical properties of the impregnated yarns and matrix and recalculate the homogenised properties of the damaged composite. These calculations may proceed for increasing loading (along a certain loading path) to calculate the non-linear behaviour of the damaged composite (Fig. 1b).
 - Calculate the homogenised properties of the composite material in undamaged or damaged state
- The output of this meso-FE modeling may be:
- Details of the stress-strain fields in the unit cell
 - Influence of details of the textile architecture on meso-scale: voids, uneven distribution of fibres inside yarns/plies, non-ideal local geometry of compacted yarns etc.
 - Stress-strain concentrations, hence strain limits for damage initiation
 - Damage development on meso-scale and deterioration of the homogenised mechanical properties

- Material models (homogenised) to be used in macro-calculations for the elastic regime and for the non-linear behaviour of the composite, for undeformed and deformed (compression, shear, biaxial tension) state.

In the following sections the stages of the “road map” are discussed in an orderly fashion.

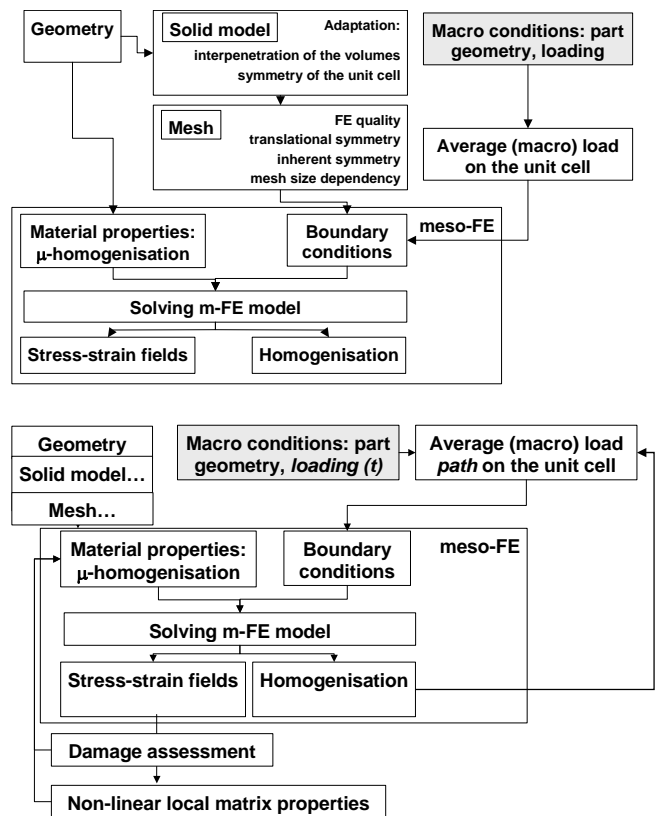


Fig. 1 “Road maps” for m-FE: (a) linear; (b) with damage

3. Transforming geometrical model into description of volumes

The geometrical and mechanical model of textiles, implemented in the software package *WiseTex*, provides a full description of the internal geometry of the following types of fabrics: 2D and 3D woven, two- and three-axial braided, knitted, multi-axial multi-ply stitched (non-crimp fabric). Input data include: (1) Yarn properties: geometry of the cross-section, compression, bending, frictional and tensile behaviour, fibrous content; (2) Yarn interlacing pattern; (3) Yarn spacing within the fabric repeat. Energy minimisation and approximations of the shape of the yarns using “anchor points” is employed to calculate the internal structure of the fabric in the relaxed state and under compression, bi- and uniaxial tension and shear. The fabric model is

comprised of yarns and (for non-crimp fabrics) of fibrous plies. The yarns are transformed into volumes for FE modelling as follows.

Fig. 2a illustrates the description of the yarns. The midline of a yarn is given by the spatial positions of the centres of the yarn cross-sections O : $\mathbf{r}(s)$, where s is coordinate along the midline, \mathbf{r} is the radius-vector of the point O . Let $\mathbf{t}(s)$ be the tangent to the midline at the point O . The cross-section of the yarn, normal to \mathbf{t} , is defined by its dimensions $d_1(s)$ and $d_2(s)$ along axis $\mathbf{a}_1(s)$ and $\mathbf{a}_2(s)$. These axes are “glued” with the cross-section and may rotate around $\mathbf{t}(s)$. Because of this rotation the system $[\mathbf{a}_1, \mathbf{a}_2, \mathbf{t}]$ may differ from the natural coordinate system along the spatial path $[\mathbf{n}, \mathbf{b}, \mathbf{t}]$.

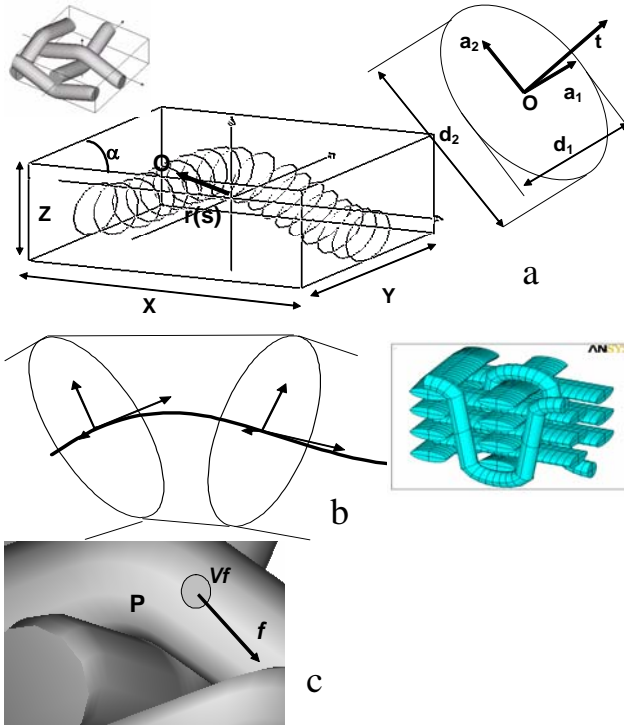


Fig. 2 Geometrical model of yarns and transformation into volumes of the solid model: (a) Cross-sections of a yarn in *WiseTex* model; (b) Building of the solid volumes and example of the solid model subdivided into volumes; (c) Properties of the fibrous assembly at a point P inside a unit cell

The shape of the cross-section can be assumed elliptical, lenticular etc. Definition of the spatial positions of a yarn with a given cross-section shape in a unit cell consists therefore of five periodic functions: $\mathbf{r}(s)$ (then $[\mathbf{n}, \mathbf{b}, \mathbf{t}]$ vectors can be calculated), $\mathbf{a}_1(s)$, $\mathbf{a}_2(s)$, $d_1(s)$, $d_2(s)$. These functions are calculated for all the yarns in the unit cell by the geometrical model. When used in numerical

calculations, all these functions are given as arrays of values for a set of points along the yarn midline, the quality of representation of the continuous yarn lines and especially the continuity of the tangent regulated by the fineness of the divisions of the yarn middle lines.

This description fully defines the volumes of the yarns in a unit cell (Fig. 2b). The format is the same for orthogonal and non-orthogonal (angle α , Fig. 2a) unit cells. The in-plane dimensions of the unit cell X , Y are given by the repeat size of the textile structure, whereas the thickness Z is calculated as the difference between the maximum and minimum z -coordinates of the cross-sections of all the yarns in the unit cell.

To describe the fibrous structure of the unit cell, consider a point P and fibrous assembly in the vicinity of this point (Fig. 2c). The fibrous assembly can be characterised by physical and mechanical parameters of the fibres near the point (which are not necessarily the same in all points of the fabric), fibre volume fraction V_f and direction f of them. If the point does not lie inside a yarn, then $V_f=0$ and f is not defined. For a point inside a yarn, the fibrous properties are easily calculated, providing that the fibrous structure of the yarns in the virgin state and its dependency of local compression, bending and twisting of the yarn are given.

The distribution of fibres over a cross-section is usually assumed uniform, and value of V_f is the same in all the points on the cross-section (but may differ from cross-section to cross-section according to the change of d_1 and d_2). Non-uniform distribution may be important for damage analysis – in this case V_f will vary over the cross-section.

4. Adaptation of the solid model and meshing

4.1. Symmetry and boundaries of the unit cell

Geometrical models of a unit cell can have correct translational symmetry properties, but may not be confined into a volume with flat facets (which will eventually be filled with matrix in FE model), which allows easy definition of loading and boundary conditions. To achieve that, the easiest way is to make a geometrical model of four unit cells, transform it into a solid model, and then, using tools of FE or CAD software, perform division operations. Fig. 3 illustrates this process, using an example of three-axial braided reinforcement. The model in the middle of Fig. 3d produces the same fabric geometry when translated periodically in two directions, as the

initial model (Fig. 3a), but it is confined into a parallelepiped. This transformation is standard for any periodic textile structure. The procedure of cutting out a repetitive element with flat facets may be especially useful in building models of layered randomly nested structures.

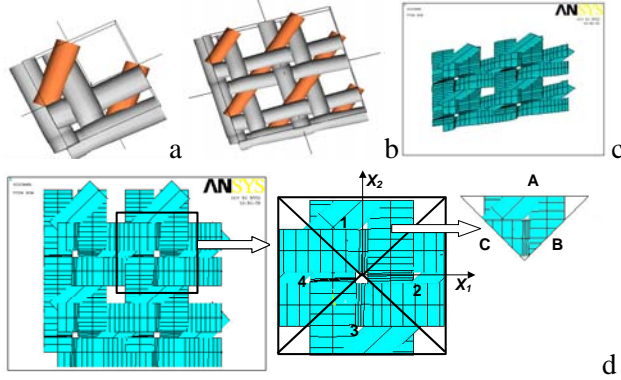


Fig. 3 Example of transformation of a solid model: three-axial braid. (a) Unit cell (*WiseTex* model); (b) Four unit cells (*WiseTex*); (c) Solid model of four unit cells in ANSYS; (d) selection of one unit cell confined into a parallelepiped and minimal unit cell

Using the inherent symmetry of a particular fabric, it is possible to reduce the size of the model. Consider the three-axial reinforcement shown in Fig. 3. $\frac{1}{4}$ of the unit cell 1 is transformed into other three quarters 2,3,4 with the following mapping:

$$1 \rightarrow 2 \text{ (rotation around the line } x_1 = x_2 \text{):} \quad (1) \\ (x_1, x_2, x_3) \rightarrow (x_2, x_1, -x_3)$$

$$1 \rightarrow 3 \text{ (rotation around the axis } x_3 \text{):} \quad (2) \\ (x_1, x_2, x_3) \rightarrow (-x_1, -x_2, x_3)$$

$$1 \rightarrow 4 \text{ (rotation around the line } x_1 = -x_2 \text{):} \quad (3) \\ (x_1, x_2, x_3) \rightarrow (-x_2, -x_1, -x_3)$$

Stress-strain fields calculated for $\frac{1}{4}$ of the unit cell is mapped over the full unit cell using equations (1-3). The symmetry equations are used to derive periodic boundary conditions for the reduced unit cell (section 5 below). We will see that using the symmetry of the unit cell may not be possible if the loading conditions do not possess the same symmetry.

4.2. Correcting interpenetrations of the yarn volumes

If the geometry for the meso-FE model is acquired by direct measurement of the yarn shapes in the

composite, then there are no defects in mutual placement of the yarn volumes. However, such approach has limited predictive capabilities. General-purpose geometrical models, like the models, discussed here, use several simplifying assumptions. One of these assumptions is a fixed shape (but maybe changing dimensions) of the yarns cross-sections. The shape of the yarn middle line prescribes the positions of the centres of the cross-sections. The model calculates dimensions of the cross-sections (d_1 and d_2 , see Fig. 2b), ensuring that the distance between the contacting yarn centre lines is equal to the sum of their dimensions.

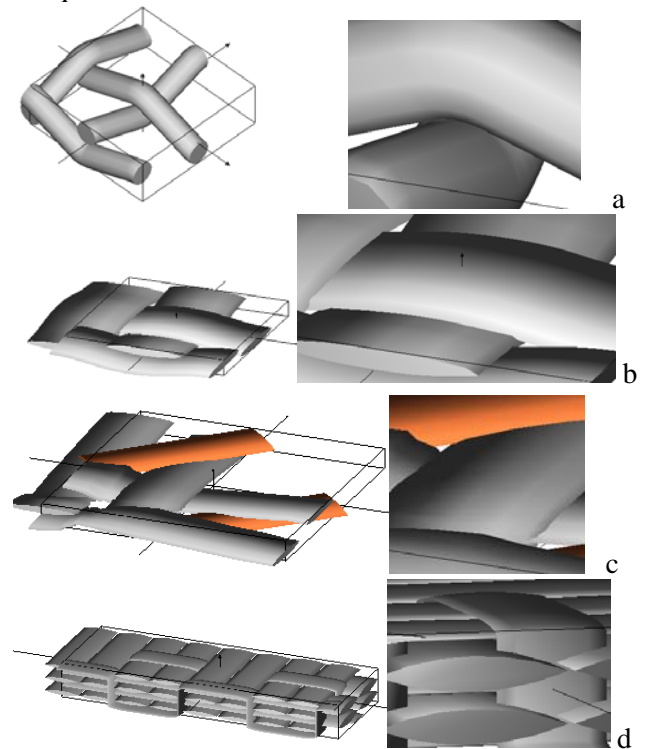


Fig. 4 Types of interpenetration of yarn volumes: (a) No interpenetration for the case of round yarns; (b) Very flat yarns; (c) Non-orthogonal configuration; (d) Very dense 3D woven fabric

For quite a wide class of woven fabrics such a treatment is sufficient to create geometrical model, which can be easily meshed in FE package. The majority of the research cited in the introduction uses such a geometry for the simple cases of not-so-tight, orthogonal 2D woven fabrics with the cross-section of the yarns either close to cylindrical or elliptical/lenticular with width-to-thickness ratio below 5...10. However, the condition of point or line contact does not guarantee that the surfaces of the contacting yarn never penetrate one another, and interpenetration may occur (Fig. 4). Three types of interpenetration could be identified:

1. Tight orthogonal structures with flat yarns. The interpenetrations occur close to the middle of the yarn width (Fig. 4b). This is the easiest case, which could be for some configurations mended using a lenticular cross-section shape or by modification of the yarn dimensions, preserving the cross-section symmetry.

2. Non-orthogonal intersections of flat yarns (Fig. 4c). Yarn edges “cut into” the intersecting yarn. This type of interaction between yarns produces local compression, which leads to non-symmetrical yarn shapes, and cannot be resolved preserving the assumption of the shape symmetry.

3. Tight placement of the yarns, especially in 3D fabrics (Fig. 4d). In reality the Z-yarn in this figure will be compressed laterally inside the fabric. This may not be accounted for by geometrical models. Whilst still usable for fibre orientation-, inclusion- or voxel-based models of micro-mechanics, such defects in the geometrical description are not likely to be corrected by any intersection algorithm. Meso-FE analysis in this case requires more precise geometry as a starting point.

The problem of interpenetration is not caused by assumptions of a particular model, but is a generic consequence of the constant shape of the yarns and limited – point or line – control of the contacts. Attempts to cope with the problem using local reduction of the dimensions of the yarns without changing the shape can solve the problem only partially, for not-so-thin cross-sections, not-so-tight fabrics and only for orthogonal intersections. The ultimate geometrical model handling the problem of volume intersections is still to be developed. This model would create yarn geometries with local deflection of cross-section shape accounting for local interactions of the yarns and accommodating accordingly the shape – non-symmetrical, freely defined by the points on the contour. The straightforward, but cumbersome way of building such a model is calculating yarn contact interactions with FE simulations of dry fabric, solving contact problems, and implementing correct mechanical behaviour in tension, compression and shear of the yarns as fibrous assemblies. Existing FE models of dry fabrics do not deal with such models. They calculate deformations of dry fabric, starting from a certain relaxed configuration, where the interpenetration should be avoided beforehand.

The approach which we propose in the present paper, exploits the idea of calculation of local compressive deformation of the yarns, but it uses this as an intermediate calculation, performed on

isolated parts of the yarns, does not use contact formulation, should be in general considered as an *ad hoc* solution and is very far from full FE analysis of the relaxed state of dry fabrics. Nevertheless, it works effectively in quite complex cases, can handle very thin cross-section shapes (width-to-thickness about 100) and is automated for a wide class of woven reinforcements, both orthogonal and non-orthogonal. The proposed algorithm creates geometries of the contacting yarns reasonably resembling the actual distortions of the regular shapes due to the contact forces. However, the rigorous comparison with the real shapes of the yarns has not yet been made (the work is on-going). The correction of the yarn volumes for a woven fabric proceeds as follows (Fig. 5).

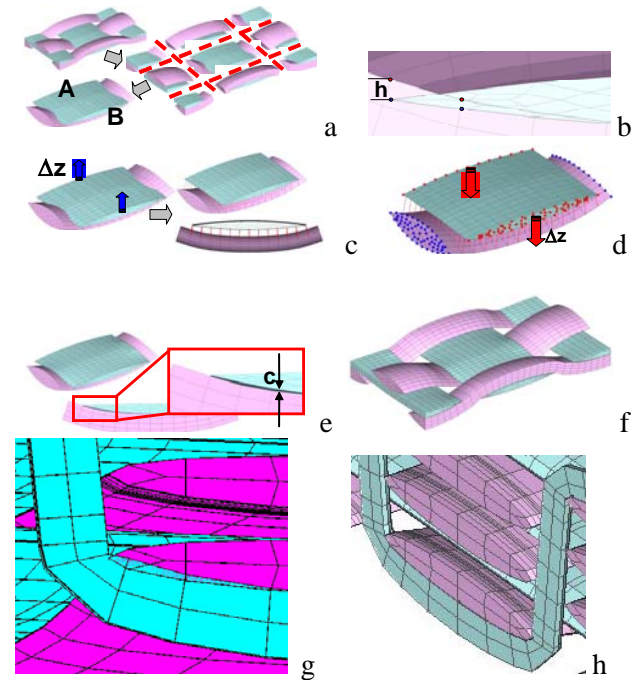


Fig. 5 Algorithm of correction of the yarn shapes: (a) Subdivision of the unit cell; (b) Penetrating yarn volumes; (c) Separation of the yarn volumes and adding beam elements; (d) Intermediate FE problem; (e) Resulting non-penetrating mesh; (f) Assembled model with non-penetrating yarns

Step 1. Preliminary meshing and division of the unit cell (Fig. 5a). The volumes of each of the yarns, exported from the geometrical model, are meshed separately. The unit cell is subdivided in a set of sub-problems, each containing one zone of the yarn contact. The division operation is crucial for the method, as it relies on having not more than one contact zone per sub-problem. The separation is done automatically, using information of the yarn

spacing and dimensions defined by the geometrical model: separation plane is positioned in the middle of the pore between the yarns.

Step 2. Analysis of interpenetrations (Fig. 5b). Consider a sub-problem. One of the contacting yarns (A, Fig. 5a) will be moved during the solution, another (B) will remain in place. For all the points in the upper boundary of the A-yarn mesh, which are situated inside another yarn, a closest boundary mesh point of the B-yarn is found, and the vertical distance h between them is stored. The two nodes of A and B mesh form a pair (P_A, P_B) .

Step 3. Separation and adding beam elements (Fig. 5c). Based on the calculated h_p , where p is the number of the point, and on the user-defined clearance c between the two yarn volumes (Fig. 5e), the separation distance is defined as

$$\Delta z = \max_p h_p + c \quad (4)$$

The volume A is moved up by Δz . Beam elements, connecting points in the pairs $(P_A, P_B)_p$, are inserted.

Step 4. Solution of the intermediate FE problem (Fig. 5d). Now the volumes A and B will be pressed together to create a non-penetrating configuration. The displacements on the cut-out facets of the volume A are assigned as $u = (0, 0, \Delta z)$, the cut-out facets of the volume B remain in place: $u = (0, 0, 0)$. The stiffness of the beam elements is given by

$$E = \begin{cases} 0, l > c \\ E_b, l \leq c \end{cases}$$

where l is the length of the beam, c is the user-defined clearance. The value of E_b is arbitrary, as well as the properties assigned to the yarn volumes; the ratio of stiffness of the yarns and E_b can be used to tune the result of the sub-modelling. The Poisson ratio for the yarn volumes is set equal to 0.5 (or just below 0.5 to avoid numerical difficulties), to preserve the yarn volume and hence the fibre volume fraction within the yarns.

The result of solving of the intermediate problem is shown in Fig. 5e. The yarn volumes are clearly separated by the clearance c , and the interpenetration is gone.

Step 5. Assembling the model (Fig. 5f). Because of the displacement conditions imposed on the cut-out facets of the yarns, after solving of the intermediate problems these facets occupy the same positions as when the division of the unit cell was performed. Hence the model is easily reassembled and is ready for addition of the matrix volume, final meshing, applying boundary conditions and solving of the

meso-FE problem for the unit cell. Fig. 5g,h illustrate the application of the automated procedure for the more difficult case of 3D woven structure.

The procedure described above is suited for automated processing. When the initial division of the unit cell is not performed easily (as this is the case for the 3-axial braid of Table 1) and manual manipulations are needed (see [1] for details).

Note that the presence of a thin layer of matrix in between the contacting yarns is important for successful meshing of the full meso-model. If this layer is absent, the touching yarn will form wedge-like volumes, produce degraded elements and will lead to numerical artefacts in the solution in this region.

4.3. Meshing

After dealing with interpenetration of volumes the model of textile composite should inherit a geometry obtained in the intermediate modelling. The latter is presented by fragmented and separated yarn geometry and mesh. The deformed FE mesh of the intermediate problem cannot be used as a mesh for the final model since the elements have changed their shape while solution and are distorted. The deformed mesh is hence transposed to the solid entities. The new volumes are generated by the deformed element configuration and then joining these volumes.

The subsequent meshing of the volumes of yarns and the matrix can be done using any meshing engine. Different strategies could be adopted: one may mesh yarn volumes first using sweeping of the planar mesh on the yarn cross-section throughout the yarn volume, and then build the mesh in the matrix, or rely on the quality of the mesh engine and ask it to mesh the whole unit cell volume automatically.

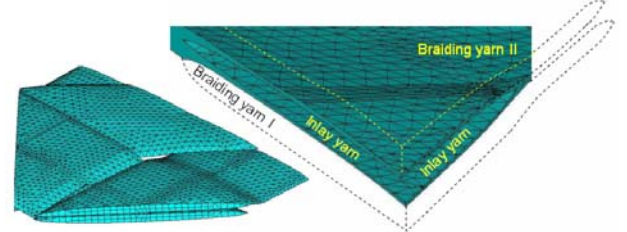


Fig. 6 3-axial braid: The mesh in the yarns and the mesh in the matrix (the dashed lines show volumes of the yarns)

The latter option (automated meshing in ANSYS) was used in the example of 3-axial braided composite (Fig. 6). The element used is a 3-D 20-node (three degrees of freedom per node) structural solid element (SOLID186 of ANSYS). It has

quadratic displacement behaviour and is recommended for modelling irregular meshes. Prism-shaped, tetrahedral-shaped, and a pyramid-shaped element are the particular cases of this element with a reduced 10-node scheme. The element shape at a place is chosen by an automatic mesh generator. Total number of elements for the quarter of the unit cell is 64,676, while node number is 83,739. 12,621 nodes are involved in the constraint equations for the symmetrical boundary conditions. Total calculation time for a linear problem was about 5 minutes on Pentium IV PC.

5. Periodic boundary conditions

The stress-strain fields in the unit cell should have the same properties of translational symmetry as the unit cell itself. If the unit cell is characterised by translation vectors \mathbf{b}_1 and \mathbf{b}_2 (Fig. 7), then these boundary points are transformed one into another by the translation

$$A' = A + \vec{b}_1, B' = B + \vec{b}_2 \quad (5)$$

Conditions of periodicity for a given average deformation tensor $\langle \underline{\varepsilon} \rangle$ (given by macro-conditions of the test or by local results of a macro-simulation) are:

$$\vec{u}(A + \vec{b}) - \vec{u}(A) = \langle \underline{\varepsilon} \rangle \cdot \vec{b} \quad (6)$$

for any point A on the boundary of the unit cell, and one of the translation vectors \mathbf{b} . Note that equation (6) can be applied to a unit cell of any shape.

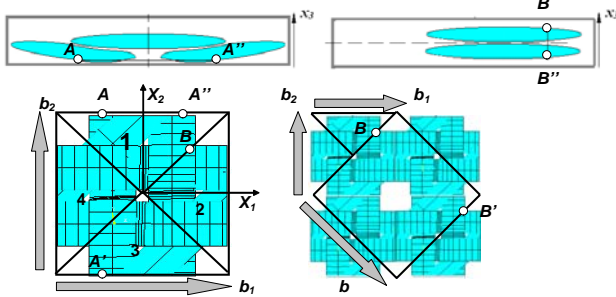


Fig. 7 Periodic boundary conditions: corresponding points for 1/4 of the unit cell

Equation (6) is easily implemented in FE packages using the apparatus of constraint equations, providing that the nodes on the opposite facets correspond one to another by (5). This means that the mesh on the opposite facets should be exactly identical, which is not necessary achieved by automatic meshing engines.

When the model is reduced using the symmetry of the reinforcement geometry, relation (6) must be rewritten. Whitcomb [3] proposed a systematic

procedure for deriving boundary conditions for partial unit cells with periodic microstructure. Application of this procedure of to the 3-axial braided composite, as shown in Fig. 7, consider first the correspondence of points on the boundaries of 1/4 of the unit cell (designated 1 in Fig. 7), imposed by the periodicity of the full unit cell. Two periodicity vectors \mathbf{b}_1 and \mathbf{b}_2 must be accounted for.

For the periodicity in direction \mathbf{b}_2 point A on the boundary of quarter of unit cell corresponds to the point A' on the opposite face of the full unit cell. Point A' is transformed into point A'' on the boundary of quarter of unit cell by symmetry transformation (2). Equation (6) is rewritten for the corresponding points as

$$u_i(A) - \gamma_A \alpha^{I3}_{ij} u_j(A'') = \langle \varepsilon \rangle_{ik} b_{2k} \quad (7)$$

where u_i are components of displacement ($i, j, k = 1, 2, 3$), repeating indices mean summation, $\{\alpha^{I3}_{ij}\}$ is the matrix of transformation of the quarters 1-3 (2), and the coefficient $\gamma_A = \pm 1$ ensures the equivalence of the stresses and strains on the symmetric boundaries of the unit cell (the notation used here is the same as in [3]). For the case under consideration (rotation by π around x_3) the sign of γ is chosen as follows:

$$\gamma_A = +1 \text{ for } \sigma_{11}, \sigma_{22}, \sigma_{33}, \sigma_{12};$$

$$\gamma_A = -1 \text{ for } \sigma_{23}, \sigma_{13}.$$

The sign of γ is +1 for components of stress/strain, which do not change their sign after applying of the symmetry transformation, and -1 otherwise.

The periodicity direction \mathbf{b}_1 presents a difficulty, as the corresponding facets of quarter of the unit cell are not on the borders of the full unit cell. To write boundary conditions for the right-bottom facet of quarter on the unit cell (point B, Fig. 7), consider another unit cell, created by translations

$$\mathbf{b} = \mathbf{b}_1 - \mathbf{b}_2$$

Point B corresponds to B' on the opposite side of this unit cell. Point B' could be considered as belonging to the quarter 1 or quarter 2. Only the second possibility allows accounting for the symmetry transformation. Point B' is transformed into point B'' on the boundary of quarter of unit cell by symmetry transformation (1). Equation (6) is rewritten for the corresponding points as

$$u_i(B) - \gamma_B \alpha^{I2}_{ij} u_j(B'') = \langle \varepsilon \rangle_{ik} b_k \quad (8)$$

where $\{\alpha^{I2}_{ij}\}$ is the matrix of transformation of the quarters 1-2 (1), and the coefficient $\gamma_B = \pm 1$ ensures the equivalence of the stresses and strains on the symmetric boundaries of the unit cell. For the case under consideration (rotation around $x_1=x_2$) the sign of γ is chosen as follows:

$$\gamma_B = +1 \text{ for } \sigma_{11}, \sigma_{22}, \sigma_{33}, \sigma_{13};$$

$$\gamma_B = -1 \text{ for } \sigma_{12}, \sigma_{23}.$$

The left-bottom face of quarter of the unit cell is treated in the same manner. Note that conditions (7) and (8), in contrast to (6), relate points on the same facet of the unit cell.

7. Material properties

Yarns and fibrous plies are locally (on the scale of one finite element) represented as an unidirectional assembly of fibres. The direction of the fibres and the fibre volume fraction are calculated by the geometrical model, accounting for the uneven distribution of fibre volume fraction in the yarns, which is an important factor for prediction of damage initiation and development.

The stiffness matrix of the material in the finite element is calculated using micro-meso homogenisation, based on empirical formulae or on micro-FE homogenisation. An example of the former are widely used formulae of Chamis:

$$E_{11} = V_f E'_{11} + (1 - V_f) E_m; E_{22} = E_{33} = \frac{E_m}{1 - \sqrt{V_f} \left(1 - \frac{E_m}{E_{22}^f} \right)} \quad (9a)$$

$$G_{12} = G_{13} = \frac{G_m}{1 - \sqrt{V_f} \left(1 - \frac{G_m}{G_{12}^f} \right)}; G_{23} = \frac{G_m}{1 - \sqrt{V_f} \left(1 - \frac{G_m}{G_{23}^f} \right)} \quad (9b)$$

$$\nu_{12} = \nu_{13} = V_f \nu_{12}^f + (1 - V_f) \nu_m; \nu_{23} = \frac{E_{22}}{2G_{23}} - 1 \quad (9c)$$

Formulae (9) were used for calculation of the local stiffness properties for the 3-axial braid modelling.

The second set of the material properties are parameters for the criterion of damage initiation, which are calculated from the strength of the unidirectional layer of fibres under different loading conditions. The difficulty here is dependency of the strength parameters on local fibre volume fraction, which may vary in a wide range (30...90%), which is not fully covered by the existing experimental data. Moreover the micro-mechanical damage theories are not fully validated for a 3D stress-strain state. Hence the assignment of the damage criterion parameters and their dependency of local fibre volume fraction is a question of “educated guess” at the present stage. In the absence of the experimental data the empirical approximate formulae can be used, as proposed by Rosen and Hirai:

$$F_L^{(t)} = F_f \cdot V_f + (1 - V_f) \cdot F_m^{(t)} \cdot \frac{E_m}{E_{fL}} \quad F_L^{(c)} = \frac{G_m}{1 - V_f \cdot \left(1 - \frac{G_m}{G_{fL}} \right)}$$

$$F_T^{(t)} = F_m^{(t)} \frac{E_T}{E_m} \cdot (1 - V_f); \quad F_T^{(c)} = F_m^{(c)} \frac{E_T}{E_m} \cdot (1 - V_f)$$

$$F_{LT} = F_{TZ} = F_{ZL} = \frac{1}{2} F_T^{(c)}$$

where F are the UD material strength, (t) stands for tension, (c) for compression; L – fibre direction, T , Z – transverse direction; m – matrix; f – fibre.

8. Homogenisation

We consider below the meso-macro homogenisation. The same may be applied to micro-meso homogenisation as well.

On the macro-scale level the composite material is considered as homogeneous, with the relation between macro strains E and macro-stresses Σ , given by

$$\Sigma_{ij} = C_{ijkl}^H E_{kl} \quad (10)$$

(here and in all the formulae in this section, the indices are in the range 1...3 and the summation rule on the repeating indexes is used; no summation on indexes in brackets). The aim of homogenisation is to find the macro-stiffness matrix C^H , to be used in macro-FE analysis. On meso-level C^H is defined by the (local) internal structure of the material and properties of the constituents.

Standard approach to the problem of homogenisation is to consider the unit cell of a textile composite as a repetitive part of an infinite array of identical cells. Then meso-FE modelling can be used to analyse the response of the material on the meso-level and to derive the behaviour (10). This formulation allows using periodic boundary conditions (6) for the meso-model. The main assumption of the approach is infinity of the medium and exact periodicity of the meso-geometry and the stress-strain fields, which allows using periodic boundary conditions (6).

These assumptions are not strictly applicable for the cases when the meso-geometry changes over a macro-part, or if there is a local change of the geometry, for example, damage. The former (differences of meso-geometry) normally happens over distances larger then several unit cells, and the periodicity can be considered as an approximation of real boundary conditions. The latter case cannot be treated that lightly, as periodicity assumes that the identical damage pattern is present in all the neighbouring unit cells, which does not agree with experimental observations.

To determine the effective properties of the periodic composite, six boundary value problems for a unit cell have to be solved denoted as (i, n) , $i, n = 1 \dots 3$. In a

problem (i,n) the macro strain tensor has only one non-zero component: $\langle \varepsilon_{kl}^{(i,n)} \rangle = E^{(i,n)} \delta_{ik} \delta_{nl}$, where $\langle \dots \rangle$ is averaging over all the elements in the unit cell, ε denotes meso-strain. The six problems to be solved correspond to $(i,n) = (1,1); (2,2); (3,3); (1,2); (2,3); (1,3)$.

As the problem is linear, the value of $E^{(i,n)}$ is of no importance; we assume below $E^{(i,n)} = 1$. The periodic boundary conditions (6) expressing continuity of the stress strain field in the periodically translated unit cells are written as follows:

$$u_k^{in}(A+b) - u_k^{in}(A) = \delta_{ik} \delta_{nl} b_l = \delta_{ik} b_n \quad (11)$$

where A and $A+b$ are the corresponding points on the boundaries of the unit cell.

After solution of each of the six meso-FE problems (i,n) the strain tensor $\varepsilon_{pq}^{(i,n)}$ is calculated for each of the final elements of the model. The effective stiffness of the unit cell C^H (10) is then calculated by averaging:

$$C_{klin}^H = \langle C_{klpq} \varepsilon_{pq}^{(i,n)} \rangle \quad (12)$$

where C is stiffness of an element.

The meso-FE analysis of 3-axial braid was performed using ANSYS and SACOM FE packages using two types of tetrahedral elements: quadratic (10 nodes) in ANSYS and linear (4 nodes) in SACOM. ANSYS calculations were done on 1/8 of the unit cell (Fig. 6), SACOM – on the full unit cell. The geometry of the mesh in both cases was exactly the same.

Table 2 Homogenised properties of the 3-axial braided composite

Test direction	Young modulus, GPa			Poisson coefficient		
	Exp.	FE	CLT	Exp.	FE	CLT
0° (machine)	32.6±1.1	35.9	36.2	0.73±0.06	0.61	0.77
45° (braiding)	36.8±1.8	38.6	44.8	0.07±0.02	0.07	0.07
90° (cross)	15.9±0.7	16.7	17.8	0.39±0.03	0.33	0.37

Table 2 shows the homogenised properties of the composite, calculated using the procedure described above. The FE-computed values (which differ for the both variants not more than ± 0.1 GPa for the stiffness and by 0.01 for the Poisson coefficient) are compared with predictions of simple laminate theory calculations and with experimental values, obtained with tensile testing of RTM-produced composite plates with four layers of the braided reinforcement. The laminate plate theory results were calculated for

a laminate consisting of four layers. Three of them are characterised with orientation and fibre volume fraction of the yarns. The relative plies thickness was chosen according to in-plane fraction of yarn volume (volume of the braiding yarns in the unit cell is 1.414 times volume of the inlays). A matrix ply was added to balance the average volume fraction. The FE analysis (with the detailed modelling of the composite geometry) and the rough laminate model give similar results for the overall stiffness values (the latter gives overestimation of the stiffness not more than 12%). The need in FE analysis mainly comes from the aim to get an adequate description of the internal strain and stress state. Laminate model is unable to estimate influence of the bridging effect, yarn interaction, non-homogeneous matrix distribution and so on.

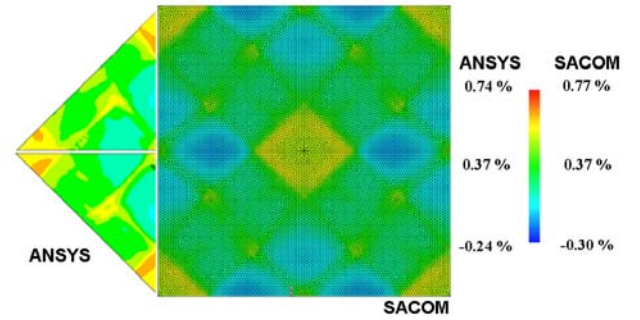


Fig. 8 Linear meso-FE analysis of 3-axial braid: comparison of the ANSYS and SACOM solutions

Once homogenised stiffness properties are defined, a tensile test is simulated (loading in machine –inlay direction). The average strain in machine direction is the governing parameter. Average strain in cross and thickness directions are set proportional to the governing strain according to the correspondent Poisson's ratios. Fig. 8 compares solutions with the two different FE software packages (ANSYS and SACOM), which are very close, and shows the deformations of the unit cell in the elastic regime. The applied strain of 0.3% corresponds to the onset of damage, registered using acoustic emission and full-field strain measurements.

9. Damage modelling

The most straightforward way for simulating damage is to base the model on fracture mechanics, directly introducing cracks in the FE model. However it is computationally difficult to introduce free boundaries in complex textile architectures. That's why only 2D or simplified geometries (mosaic model) were tried in the framework of classical fracture mechanics. Direct crack modelling requires a well defined crack path, which is only

known in the case of delaminations. Shear lag models are known to provide reasonable prediction of the degraded stiffness, however these models require a dependence of crack density on applied strain to be known; the latter seems not to be invariant characteristics for the textile structures.

Damage mechanics approach, which is based on damage variables without introducing cracks directly into the mesh, uses well established failure criteria and relatively simple tests on strength of unidirectional composites as an input data. Furthermore the modelling doesn't require rebuilding mesh used for an elastic analysis, and thus it is computationally simple. The reader is referred to [1] for the detailed discussion, formulae and references. Here we present the results for the 3-axial braided composite.

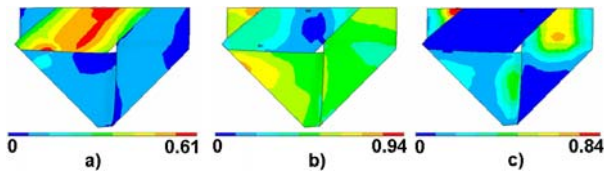


Fig. 9 Stress index I 3-axial braided composite under tension in the machine direction, applied strain 0.3%: (a) longitudinal H_L ; (b) transverse H_T ; (c) shear H_{LT}

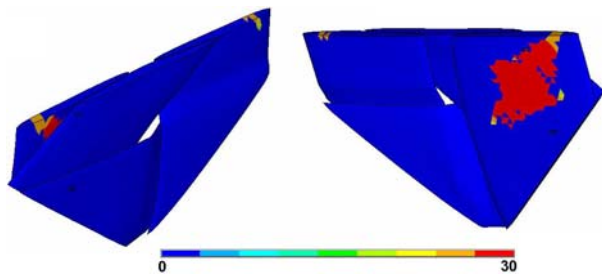


Fig. 10 Damage development in 3-axial braided composite: scale defines load step when damage occurs; maximum corresponds to the earliest stage.

As mentioned before, acoustic emission, full-field strain measurements and X-ray investigation indicate onset of damage in the 3-axial braided composite under tension in the machine direction at the applied strain of 0.3%. Fig. 9 shows the stress indices according to the Hoffman criterion. The maximum value of the index $H_T = 0.94$, hence the applied strain of 0.3% is close to the theoretical damage initiation strain. The damage is caused by transversal tensile stresses. Fig. 10 shows that the damage starts in the braiding yarn, lying at 45° to the loading direction, which corresponds to the X-ray observation of the damage.

Good predictions of the onset of damage in textile composites (analogue to the “first ply failure” in laminates) has been shown in a number of publications. We have calculated the damage onset threshold in the 3-axial braided composite for the following variants: (1) ANSYS and SACOM calculations with quadratic and linear elements correspondingly; (2) mesh finesse (number of elements) different by a factor of 2. For all the variants the damage initiation strain, predicted by Hoffmann criterion, varied in the range of $0.3 \pm 0.02\%$. This shows robustness of the damage detection algorithm.

However, when it comes to the damage propagation, the calculations show non-physical behaviour (Fig. 10). The damage propagates *along* the yarn, in the direction of the fibres, as one expects and as it is observed in experiments, but it also propagates *across* the yarn, suggesting a multitude of micro-cracks, which is not observed in experiment (there are one-two well-separated cracks over the whole yarn width). This seems to be a common drawback for meso-FE modelling of damage which use local damage criteria and properties degradation scheme, as the same effect is observed in calculation reported in literature. The effect is now a subject of our research.

10. Conclusions

We have presented an orderly approach to meso-FE modelling of textile composites. It makes clear that integrated modelling systems are in the order of the day, being ready to emerge in the coming years. Such a system will be suitable not only for academic research and illustration of principles, but also for serious treatment of practically important textile composites with complex architecture, and allowing rapid variation of the reinforcement structural parameters and mechanical properties of the constituents, using user friendly interface and adequate results both for linear and non-linear, damaged behaviour. An integrated FE-modeller should include the following modules:

- A *geometric modeller*, which defines the volumes of yarns and fibrous plies in the unit cell of textile composite, local fibre parameters on the micro-scale and provides interface with FE package to export these data;
- A *geometry corrector*, which adapts the geometrical model for requirements of the meshing engine and the particular necessities of boundary conditions formulation process;
- A *meshing engine*;

- A *material property processor*, which assigns material properties to volumes/elements, using local fibre assembly parameters on micro-scale, provided by the geometrical model, and applying a certain model of homogenisation on micro-level, or even a menu for user choice of such a model;
- *Boundary conditions routines*, facilitating posing periodic boundary conditions;
- A *FE solver and post-processor*;
- A *homogenisation engine*, which automatically applies the necessary loading and boundary condition, processes the results and outputs homogenised meso-stiffness matrix of the textile composite;
- A *damage detection processor*, employing one of (user-chosen) damage initiation criteria;
- A *damage development processor*, responsible for monitoring the damage tensor, change of the homogenised (on micro-level) properties and decisions on the damage propagation modelling.

Based on the geometrical modeller *WiseTex*, commercial ANSYS and custom-developed SACOM FE packages, we have developed an integrated system, which includes all the modules, listed above. They constitute a solid basis for future work, leading to meso-FE modelling systems, integrated with macro-FE structural analysis and μ -FE analysis of fine features of damage.

Acknowledgments

The work in K.U.Leuven was supported by European Commission (ITOOL project), government of Flanders (IWT-GBOU project "Predictive tools for permeability, mechanical and electro-magnetic properties of fibrous assemblies") and the Research Council of K.U.Leuven (OT project "Concurrent multi-scale design/engineering of textile composites" and East-European PhD grant of D.S.Ivanov).

References

- 1 Lomov, S.V., D.S. Ivanov, I. Verpoest, M. Zako, T. Kurashiki, H. Nakai, and S. Hirosawa Meso-FE modelling of textile composites: Road map, data flow and algorithms. *Composites Science and Technology*, 2007; **67**: 1870-1891
- 2 Verpoest, I. and S.V. Lomov Virtual textile composites software WiseTex: integration with micro-mechanical, permeability and structural analysis. *Composites Science and Technology*, 2005; **65**(15-16): 2563-2574

- 3 Whitcomb, J., C.D. Chapman, and X. Tang Derivation of boundary conditions for micromechanics analyses of plain and satin woven composites. *Journal of Composite Materials*, 2000; **34**(9): 724-747